

Platinum (II)-coordinated *Portulaca oleracea* polysaccharides as metal-drug based polymers for anticancer study

Qianqian Han^{a,b}, Lirong Huang^c, Ying Wang^{a,b}, Shixin Sun^{a,*}, Hao Huang^a, Fei Li^a,
Fangtian Wang^a, Ligen Chen^d, Hongmei Zhang^{a,*}, Yanqing Wang^{a,*}

^a Institute of Environmental Toxicology and Environmental Ecology, Yancheng Teachers University, Yancheng City, Jiangsu Province, 224051, People's Republic of China

^b Chemistry and Chemical Engineering, Nanjing University of Technology, Nanjing City, Jiangsu Province, 210009, People's Republic of China

^c Cardio-Thoracic Surgery, Yancheng First People's Hospital, Yancheng, 224006, People's Republic of China

^d Department of Bioengineering School of Marine and Bioengineering, Yancheng Institute of Technology, Yancheng, 224054, People's Republic of China

ARTICLE INFO

Keywords:

Portulaca oleracea polysaccharides
Alendronate
Platinum-based conjugates
Antitumor activity
Immunocompetence

ABSTRACT

Novel polysaccharide-platinum conjugated polymers bearing alendronate on *Portulaca oleracea* polysaccharides (PPS) were designed and synthesized. Their chemical structures and properties were characterized by Fourier transform infrared spectroscopy (FT-IR), ¹H NMR and ³¹P NMR spectroscopy, Thermogravimetric analysis (TGA), X-ray powder diffraction (XRD), UV-vis spectrophotometer (UV-vis) and other analysis methods. The results demonstrated that alendronate can be used as the linker of *Portulaca oleracea* polysaccharides and platinum compounds. *Portulaca oleracea* polysaccharides-alendronate (PPS-ALN) conjugates exhibited stronger antioxidant ability than PPS. The cytotoxicity assay to cancer cells was tested in vitro, and the *Portulaca oleracea* polysaccharides-alendronate-platinum (PPS-ALN-Pt) conjugates strongly inhibited the proliferation of cancer cells than PPS and PPS-ALN. The evaluation of complexes affinity toward supercoiled plasmid DNA, displayed a high DNA interaction. Interestingly, the platinum conjugates displayed immunological competence in HeLa cells by cellular immunofluorescence assay. Besides, the cellular platinum accumulation of PPS-ALN-Pt conjugates was higher than that of cisplatin in HeLa cells, implying that the polysaccharide-platinum conjugated polymers might have a synergistically therapeutic application in metal anticancer drug delivery.

1. Introduction

Cancer is one of the diseases that seriously threaten human health, and has been intimately and considerably concerned by researchers. Cisplatin is a kind of critical anticancer drugs, which has potent effects on a variety of solid tumors [1,2]. However, the severe side effects of cisplatin have limited its clinical application, which led to the development of platinum-based alternative strategies [3,4]. Polymer-drug delivery has been widely used and applied (e.g. hydrophobic drugs, amphiphilic copolymers) [5,6]. Polymer-drug delivery systems can enhance the transport efficiency of loaded drugs to solid tumors [7], as the enhanced permeability and retention effect can prolong the blood circulation and selectively distribute the delivered drugs in the organism, thereby reducing the side effects [8–10].

Moreover, Pt-based anticancer drugs constitute polymer-drug delivery which can lessen the platinum-based antitumor drugs toxicity in the process of delivery to healthy organs and prove the feasibility of this

method in the literature [11–13]. Polymer drug sustained-release systems have always attracted the attention of researchers and are at the forefront of scientific and technological progress [14–16]. Polysaccharide biodegradable polymer composites are widely used to controllably transmit and release of medicinal polysaccharides at specific locations via spontaneous reactions according to the signals generated under external conditions [17–19]. It possesses several advantages (e.g. pH-responsive release, biocompatibility, targeting) compared with other drug delivery methods, especially in the aspect of targeted drug delivery, and can release drugs according to the physiological environments [20–22].

Portulaca oleracea is an annual plant with outstanding medicinal and nutritional values widely distributed in tropical-temperate regions [23]. There are multiple biological and active substances in *Portulaca oleracea* after purification, including *Portulaca oleracea* polysaccharides (PPS) which is one of the major bioactive components of the traditional Chinese herb *Portulaca oleracea*. A kind of plant medicine of PPS apply for

* Corresponding authors.

E-mail addresses: asunshixin@163.com (S. Sun), hxzhm@126.com (H. Zhang), wuyqing76@126.com (Y. Wang).

<https://doi.org/10.1016/j.colsurfb.2021.111628>

Received 30 August 2020; Received in revised form 15 January 2021; Accepted 13 February 2021

Available online 18 February 2021

0927-7765/© 2021 Elsevier B.V. All rights reserved.

the diagnosis and treatment of dysentery, eczema, erysipelas or used as antipyretic or germicidal agent. PPS also exhibits a wide range of biological effects, including strong antioxidant effect [24], antiviral effect [25], immunomodulatory effect [26], anti-microbial activity [27], and anticancer effect [28,29].

Nowadays, more and more attentions have been paid to the application of natural products. PPS is natural plant polysaccharides with extensive pharmacological effects. However, only few reports of the preparation of new chemotherapy drugs and the formation of drug delivery systems using *Portulaca oleracea* polysaccharides as the carbon skeleton. In addition, PPS modified with sulphate is more cytotoxic to tumor cells (such as HeLa and HepG2 cells) in vitro than PPS. In general, PPS has potential application in cancer treatment [30,31].

In this work, hydroxyl groups in PPS were oxidized to form aldehydes, and then reacted with the amino group in alendronate (ALN) to form Schiff base. As shown in Scheme 1, the bisphosphonate acid group of ALN was coordinated with the platinum precursor [Pt(NH₃)₂(OH)₂] in aqueous solution to prepare new platinum-based polysaccharide drugs (PPS-ALN-Pt conjugates). Multiple analysis means were used to characterize the above samples. The antitumor activity and antioxidant activity of the conjugates were respectively studied using MTT assay, DPPH and ABTS assays. The interaction between PPS-ALN-Pt conjugates and DNA was confirmed by gel electrophoresis. This may provide a new system for cisplatin delivery.

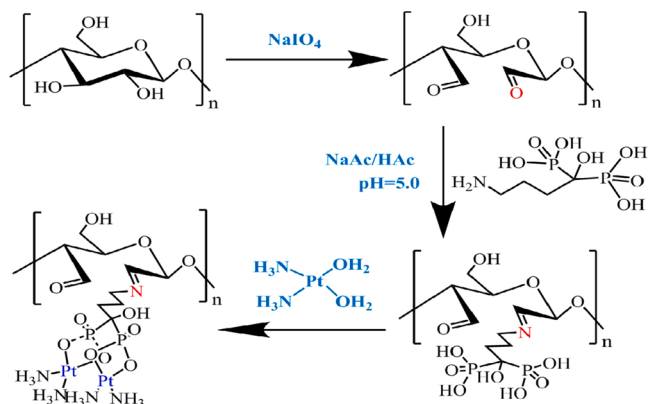
2. Materials and methods

2.1. Materials

Alendronate sodium trihydrate (ALN·3H₂O, > 97 %), sodium periodate (NaIO₄), hydroxylammonium chloride (NH₂OH·HCl), cisplatin, triethylamine (TEA), and 3-(4, 5-dimethyl-thiazol-2-yl)-2,5-diphenyl-tetrazolium bromide (MTT, ≥ 97.0 %) were obtained from Aladdin (Shanghai, China). Silver nitrate (AgNO₃) were obtained from Sinopharm Chemical Reagent Co., Ltd. Dulbecco's Modified Eagle's Medium (DMEM), RPMI-1640 medium (RPMI), penicillin/streptomycin were procured from Biyuntian Biotechnology Co., Ltd. Supercoiled pUC19 DNA/*MspI* (*HpaII*) Marker were obtained from Thermo Fisher Scientific (USA). *Portulaca oleracea* polysaccharides (PPS) (purity, 50 %) was provided from Ciyuan Biotechnology, Shanxi. Anti-Calreticulin antibody and Alexa Fluor® 488 were supplied from Abcam (Shanghai) Trading Co., Ltd. Other chemical reagents were used within the allowable dose range.

2.2. Preparation of oxidation of PPS (PPS-CHO) and phosphorylated

Portulaca oleracea polysaccharides (5 g, purity 50 %) was weighed accurately, dissolved in 110 mL deionized water, filtrated with pressure



Scheme 1. The synthesis process of PPS-ALN-Pt conjugates.

reduction, loaded into a dialysis membrane (MWCO: 3500 Da), dialyzed in 2 L deionized water for 3 days, changed the water three times per day to remove small molecules of flavonoids and acids and so forth, and removed solid impurities by centrifuging at 8000 rpm for 15 min and then filtrating under reduced pressure. The dialysate was stored in a freeze-dried bottle in a refrigerator at $-20\text{ }^{\circ}\text{C}$ for at least 4 h and then be lyophilized at $-55\text{ }^{\circ}\text{C}$ to obtain the pretreated *Portulaca oleracea* polysaccharides, storing the dried sample at $4\text{ }^{\circ}\text{C}$.

Oxidized *Portulaca oleracea* polysaccharides (PPS-CHO) were prepared according to the reported method with minor modifications [32, 33]. An aqueous solution of sodium periodate (1.8 g, 160 mL) was dropped into the purified PPS (1.5 g, 140 mL) solution dropwise. The reaction was mixed in the dark at $40\text{ }^{\circ}\text{C}$ for about 48 h, quenched by ethanol and then stirred for another 1 h. The reaction solution was transferred into a dialysis bag (MWCO: 3500 Da) and dialyzed in deionized water for 72 h to remove the unreacted substance, wadding product was obtained by freeze-drying. Hydroxylamine hydrochloride/sodium hydroxide (NH₂OH·HCl/NaOH) titration method was determined for the quantitative determination aldehyde group content of PPS-CHO which was 1.9 mmol/g according to the reported method [34].

2.3. Synthesis of PPS-ALN conjugates

PPS-ALN (*Portulaca oleracea* polysaccharides-alendronate) conjugates were prepared via the Schiff ; base reaction. PPS-CHO (0.5 g) and alendronate sodium trihydrate (0.623 g) were completely dissolved in 45 mL and 30 mL HAc/NaAc (0.1 M) buffers with the pH value at approximately 5.0, respectively. Alendronate sodium trihydrate solution was slowly dripped into a round bottom flask containing PPS-CHO solution and stirred in the dark under nitrogen protection at $50\text{ }^{\circ}\text{C}$ for 48 h. After the reaction, the solution was used in distilled water with dialysis bag (MWCO: 3500 Da) for 3 days [35,36].

2.4. Preparation of aquatic cisplatin complexes [Pt(NH₃)₂(OH)₂]²⁺

The aquatic cisplatin complexes were prepared according to previous reports with slight modifications [37]. Cisplatin (50 mg, 0.168 mmol) solution and silver nitrate (57 mg, 0.333 mmol) were stirred by overnight in the dark at room temperature, obtained an aquatic cisplatin complexes solution. After the reaction, the solution was filtered out by centrifugation (10,000 rpm, 1 h) and then was precipitated with $0.45\text{ }\mu\text{m}$ water phase filter to remove the fine silver nitrate precipitate. The acquired solution was stored at $4\text{ }^{\circ}\text{C}$ and protected from light with tin foil for short-term using.

2.5. Synthesis of PPS-ALN-Pt conjugates

PPS-ALN conjugates were soluble in 20 mL deionized water, to which TEA was added, to give a weak alkaline solution. The above aquatic cisplatin complexes was added dropwise to the prepared conjugates solution, stirred it by nitrogen protection in the dark at $37\text{ }^{\circ}\text{C}$ for 48 h. The conjugated solution was loaded into a dialysis bag (MWCO: 3500 Da) and then was dialyzed with periodically changed deionized water for 3 days. The solution was lyophilized at $-55\text{ }^{\circ}\text{C}$ to obtain dry powder which was stored into a brown bottle at $4\text{ }^{\circ}\text{C}$ and the above synthesis steps can be repeated. The Pt contents of PPS-ALN-Pt conjugates were determined by ICP-OES (Perkin Elmer, Optima 4300 DV, USA), which value was 15.94 % in average value of three times determinations. Afterwards, the synthesized samples were used for the later experiments.

2.6. Characterization

The FT-IR spectra were measured on a spectrometer (Bruker, VERTEX 80/Raman II, Switzerland) at selected wavenumber in a range from $4000\text{ to }500\text{ cm}^{-1}$ at room temperature and 40 % RH. ¹H NMR spectra

were recorded using a Bruker AVANCE III HD 400 MHz (Germany) with D₂O as the solvents. ³¹P NMR spectra were measured using a Bruker AVANCE III HD 500 MHz (Germany). UV-vis absorption standard curve experiment of a phosphate group and free radical scavenging assays were conducted on a LAMBDA 35 spectrophotometer (Perkin Elmer Ltd., USA) at 25 °C. The TGA curves of samples were performed by a thermal gravimetric instrument (STA449F5 Jupiter, Germany) which set temperature in a range from 25 to 850 °C under dynamic argon with a heating rate of 10 °C/min. The XRD patterns was measured on a diffractometer (Malvern Panalytical X'Pert³ Powder X-ray Diffractometer, Netherland), on which samples were observed at a speed of 5°/min with the scanning range of 2θ (5 to 80°) and operated in continuous mode.

2.7. Determination of phosphate radical content in PPS-ALN-Pt conjugates

Firstly, the measurement procedure of the phosphate radical standard curve was based on the report with some modifications [38]. The concentration of phosphate standard radical liquid was purchased from Aladdin (Shanghai, China) and diluted from 1 mg/L to 0.1 mg/L. The scheme firstly obtained a Tris buffer solution which MgCl₂·6H₂O (120 mg) and trimethyl aminomethane (Tris, 3.6 g) were completely soluble in 300 mL double-distilled water (DDIW), and then the value of pH was adjusted to 7.0 with HCl (1 M). The formulation of quantitative phosphorus reagent was obtained by mixing an equal volume of 3 M H₂SO₄ solution, 20 % ascorbic acid solution and 3% ammonium molybdate solution evenly. 0, 0.50, 1.00, 1.50, 2.00, 2.50, 3.00, 3.50, 4.00, 4.50 and 5.00 mL of the double-distilled water was accurately supplemented into the polyethylene tube, and standard phosphate solution (0.1 mg/mL) was then injected until the total volume to 5 mL. Tris buffer solution (3 mL) was added into each tube. After the solution of tube was slowly shaken up, it was immediately added quantitative phosphorus reagent (3 mL) and treated with a water bath at 45 °C for 0.5 h. The absorbance of the solution at 580 nm (A₅₈₀) was measured after cooling to room temperature [39]. The standard curve of phosphate radical was established between A₅₈₀ and phosphate radical concentration.

The molybdenum blue colorimetry was applied to determine the radical phosphate content of the sample [38]. PPS-ALN-Pt conjugates (0.1 g) was dissolved in a tube with concentrated sulfuric acid (1 mL) and dense nitric acid (1 mL), and then the solution was heated until smokeless. The solution was cooled and then was added into 30 % H₂O₂ aqua solution (1 mL) for one more slow heating. Above steps were duplicated until no smoke appeared in the conical flask, and the solution was currently pale yellow or colorless. After adding hydrochloric acid (6 M, 1 mL) in the conical flask, the powder sample was heated to complete decomposition. Afterwards, the above solution was shifted in a volumetric flask (50 mL) and fixed the volume with DDIW. The absorbance of the solution at A₅₈₀ was detected by a UV-vis spectrophotometer (PerkinElmer Lambda 365, USA). With the standard curve obtained by the above means, the content of phosphate radical was figured out.

2.8. Determination of degree of substitution (DS)

The degree of substitution (DS) that is assumed as the average number of a phosphate group (-PO₃H₂) on each sugar residue can be calculated by the formula Eq. (1):

$$DS = (162 + M) \times C / (M + C) \quad (1)$$

Where 162 is the relative molecular mass of one monosaccharide residue, M stands for the molar mass of substituent (-PO₃H₂), and C is the content of PO₄³⁻.

2.9. Radical scavenging activity

2.9.1. ABTS radical scavenging assessment

ABTS free radical cation (ABTS⁺) was produced by a chemical oxidation reaction with potassium persulfate, followed by the method of previous literature [40]. ABTS⁺ was generated by mingling an equal volume of 0.662 mg/mL potassium persulfate solution and 3.84 mg/mL ABTS aqueous solution, allowing the reaction laid aside in darkness for 12~16 h at room temperature. Afterwards, 2.0 mL of the reaction mixture solution was fixed in a volumetric flask (50 mL) with deionized water to obtain the working solution. Aqueous solutions of PPS, ALN, PPS-ALN and PPS-ALN-Pt conjugates with different concentrations from 0 to 0.10 mg/mL were dissolved in deionized water (2 mL). They were mixed with freshly prepared ABTS⁺ solution (2 mL), which was incubated in the dark at room temperature for 5 min. The absorbance of the resulting solution was determined by a UV-vis spectrophotometer (PerkinElmer Lambda 365, USA) at 734 nm. Three sets of parallel experiments were conducted, and the data were averaged three times. The percentage of ABTS radical scavenging effect is counted using Eq. (2).

$$\text{Scavenging effect (\%)} = (1 - A_{\text{sample}} / A_{\text{blank}}) \times 100 \% \quad (2)$$

Where A_{blank} is the measured absorbance value of ABTS free radical solution and A_{sample} is the measured absorbance value of the sample mixed with ABTS free radical solution.

2.9.2. DPPH radical scavenging assessment

The antioxidant capacity of PPS, ALN, PPS-ALN and PPS-ALN-Pt conjugates was monitored using DPPH assay [41]. The sample solutions of PPS, ALN, PPS-ALN and PPS-ALN-Pt conjugates from 0 to 0.20 mg/mL were dissolved in deionized water (2 mL) and then were mixed with freshly prepared DPPH (2 mL, 0.05 mg/mL) ethanol solution. The solutions were sufficiently shaken up and reacted for 30 min in the dark at room temperature. The absorbance of the resulting mixed solution was determined by a UV-vis spectrophotometer (PerkinElmer Lambda 365, USA) at 517 nm. We conducted three sets of parallel experiments, and the data were averaged three times. The scavenging effect of DPPH free radical scavenging effect is counted by Eq. (2), where A_{blank} is the measured absorbance value of DPPH free radical solution and A_{sample} is the measured absorbance value of the sample mingled with DPPH solution.

2.10. Cell culture and cytotoxicity assay

The relative cytotoxicity of PPS, ALN, cisplatin, PPS-ALN and PPS-ALN-Pt conjugates was tested on the HeLa, MCF-7, LO-2, and A549 cells expressed by the half-maximal inhibitory concentration (IC₅₀). The cell viability of four cells to cytotoxicity was determined by MTT assay [42]. HeLa, MCF-7, LO-2, and A549 cells were seeded in RPMI 1640 or DMEM medium containing with 10 % fetal bovine serum (FBS), 100 U/mL penicillin/streptomycin, and incubated in a constant temperature containing 5% CO₂ incubator at 37 °C. The cells were seeded in the 96-well plates contained 3500 cells of per well, which was cultured for 24 h at 37 °C. Then medium in the 96-well plates switched with fresh medium. Cells were treated with PPS, ALN, cisplatin, PPS-ALN and PPS-ALN-Pt conjugates medium solution in gradient concentration, respectively, incubated at 37 °C.

After incubation for 48 h, the cells were cultured by adding MTT solution (20 μL, 5 mg/mL in PBS) in each well and subsequently incubated for 4 h at 37 °C. It was necessary to carefully suck out the culture solution in each hole owing to terminate the culture. The cells precipitate in the 96-well plates were dissolved by dimethyl sulfoxide (200 μL), which was shaken well and immediately measured with the absorbance of 490 nm (OD₄₉₀). The absorbance of samples at 490 nm (OD₄₉₀) was detected by a microplate reader (Spectra Max M5, Molecular Devices Company, USA). The evaluation of cell cytotoxicity is calculated

according to the formula Eq. (3):

$$\text{Cell viability (\%)} = (\text{OD}_{\text{sample}} - \text{OD}_{\text{blank}}) / (\text{OD}_{\text{control}} - \text{OD}_{\text{blank}}) \times 100 \% \quad (3)$$

Where the sample is the presence of the drug sample, and the blank is the absence of the drug sample.

2.11. Agarose gel electrophoresis assay

DNA is deemed as the major target of platinum-based compounds, and therefore the interaction between PPS-ALN-Pt conjugates and supercoiled pUC19 DNA was studied by gel electrophoresis with ethidium bromide as the probe [43]. The molecular weight of supercoiled pUC19 plasmid DNA is 1.74×10^6 Da, containing 2686 base pairs. The concentration of the corresponding nucleotide is calculated as 696 μM according to the conversion formula, and the formal drug to nucleotide molar ratios (r_1) varied from 0.2 to 1.4. The supercoiled pUC19 DNA (200 ng) and different concentrations of PPS-ALN-Pt conjugates dissolving in Tris-HCl/NaCl buffers (50 mM, pH = 7.4) were formed as the sample solution until total volume reached 10 μL , which was incubated at 37 °C for 1 day in the dark. After incubation, all reactions were quenched by adding $5 \times$ loading buffer (bromophenol blue, 2 μL). The samples were loaded on a 1% agarose gel-forming electrophoresis and conducted at 90 mV for 2 h in TAE buffers (40 mM Tris-acetate, 1 mM EDTA). The agarose gel was stained with ethidium bromide solution (0.5 $\mu\text{g}/\text{mL}$) for 5 min and visualized by UV Transillumination (American, BIO-RAD ChemiDoc™ XRS + gel imaging system).

2.12. Nuclear staining assay

In the tested cells of MTT assay, the values of cisplatin and ALN for HeLa cells were the smallest, and the IC_{50} values of the four substances decreased significantly. Therefore, in the subsequent bioassay experiments, we chose HeLa cells as studying cells.

HeLa cells were grown in a 6-well cell culture plate containing chemotherapy drugs, and cultured for 24 h. Then, the medium was removed from the 6-well plate, and HeLa cells were gently rinsed with cold PBS. After trypsin treatment, the cells were harvested. HeLa cells were washed twice with cold PBS, fixed with 4% paraformaldehyde for 10 min at room temperature, and dyed with 20 μL of Hoechst 33,342 for 15 min. Ultimately, HeLa cells were washed with PBS for twice to remove the probe residue. The cell nucleus images were immediately observed and captured through an inverted fluorescence microscope (LEICA M165 FC, Germany).

2.13. Cellular immunofluorescence assay

HeLa cells were selected and treated with chemotherapy drugs. The distribution of calreticulin in HeLa cells were detected by immunofluorescence assay [46]. HeLa cells were cultured in DMEM medium. When the cell density was about 50~60 %, the PPS, ALN, cisplatin, PPS-ALN and PPS-ALN-Pt conjugates was added and cultured continuously for 24 h. The IC_{50} value of each sample was taken as the final concentration of each sample according to the MTT experiment. Then the culture solution was taken out from a 20 mm laser scanning confocal culture dish, washed with PBS, and covered with 4% polyformaldehyde for 20 min, rinsed three times in PBS for 5 min. Samples were permeabilized with 0.1 % Triton X-100 for 10 min, washed third in PBS for 5 min. Then, 5% BSA was blocked for 1 h, and 1/500 anti-Calreticulin antibody was incubated. After the first anti incubation, samples were rinsed three times in PBS for 5 min. Subsequently, goat antibody to Rabbit IgG (Alexa Fluor® 488) was cultured for 1 h carrying fluorescent markers, and DAPI was applied to label the nucleus [45]. Images were acquired on a Zeiss confocal microscope (LMS710, Germany), using the Zen™ 178 software manipulated pictures.

2.14. Cellular Pt uptake and DNA platination

HeLa cells were selected for uptake studies and cultured in a 6-well plate (Corning) at a density of 10^5 cells/mL, and incubated for 24 h under standard growth conditions. The culture medium in 6-well plate switched with fresh growth media. Meanwhile, the cells were treated with cisplatin (45 $\mu\text{g}/\text{mL}$) and PPS-ALN-Pt conjugates (284 $\mu\text{g}/\text{mL}$) in fresh growth media for 24 h [46]. HeLa cells were harvested and washed twice with PBS (4 °C), and then were digested with concentrated nitric acid (100 μL) for 2 h at 95 °C, followed by adding hydrogen peroxide (30 %, 50 μL) and hydrochloric acid (50 μL) at 95 °C to give a thoroughly homogenized solution [47]. Water was then added to dilute the solutions until to 1 mL, and the Pt content was determined by ICP-MS using a standard Plasma-Quad II instrument (VG Elemental, Thermo Optek-Corp). The average of three groups of repeated experimental data was regarded as the final result.

3. Results and discussion

3.1. FT-IR analysis

Fourier transform infrared spectroscopy (FT-IR) was applied to recognize the types of functional groups in the material. The FT-IR spectra of PPS, PPS-CHO, ALN, PPS-ALN and PPS-ALN-Pt conjugates were schematized in Fig. S1. As shown in Fig. S1(A), the band observed at $3500\sim 3200 \text{ cm}^{-1}$ and $2995\sim 2839 \text{ cm}^{-1}$ was belonged to the -OH group stretching vibration, as well as the -CH₃ and -CH₂ groups stretching vibration, respectively. The emerging characteristic absorption peak of PPS-CHO at 1725, 1455, 1322, 1275, 1112 cm^{-1} were found in FT-IR spectra. NaIO₄ was utilized for oxidizing two adjacent hydroxyl groups in sugar ring to the aldehyde group [48]. The new peak of 1725 cm^{-1} (CO=) was assigned to the aldehyde group in PPS-CHO, which demonstrated that PPS were successfully oxidized as shown in Fig. S1(A). The -C=N- stretching vibration peak of PPS-ALN conjugates at 1641 cm^{-1} overlapped with other functional groups in PPS-CHO that cannot be discerned shown in Fig. S1(B). However, the characteristic peaks of P=O or P-O-C from 1152 and 924 cm^{-1} indicated that PPS-ALN conjugates was successfully synthesized [49]. The vibrational peak of functional groups about 1322 and 537 cm^{-1} of PPS-ALN-Pt conjugates spectra was broadened, which belonged to -N-H- stretching vibration. It was preliminarily proved that the platinum complex grafted onto PPS-ALN-Pt conjugates by coordination.

3.2. ¹H NMR analysis

The ¹H NMR spectra of PPS, PPS-ALN and PPS-ALN-Pt conjugates dissolving in D₂O were indicated in Fig. 1(A). It can be seen from the ¹H NMR spectra of PPS that the signals at 4.0~5.0 ppm and 5.0~5.6 ppm belonged to β -configuration and α -configuration glucose, respectively. The signal peak at approximately 1.88 ppm and 1.75 ppm in the ¹H NMR spectrum was the characteristic peak of the methylene group protons of -CH₂CH₂C(OH)(PO₃H₂)₂ in ALN of PPS-ALN and PPS-ALN-Pt conjugates [50]. As depicted in ¹H NMR spectra of PPS-ALN-Pt conjugates, the appearance of proton peaks at approximately 1.83 ppm and 1.11 ppm was characteristic peak of the methylene group protons and amino hydrogen, indicated that PPS-ALN-Pt conjugates were successfully synthesized by coordination of platinum complex with biphosphate.

3.3. ³¹P NMR analysis

The formation of the complex conjugate was confirmed by ³¹P NMR (500 MHz, D₂O or DMSO-d₆) [51,52]. ³¹P NMR spectra of ALN, PPS-ALN and PPS-ALN-Pt conjugates were characterized and shown in Fig. 1(B). The water solubility of ALN is 5 mg/mL. In order to make the phosphorus spectrum better presented, 10 mg of ALN was dissolved with DMSO-d₆ (600 μL). The ³¹P NMR spectra of ALN was the signal peaks at

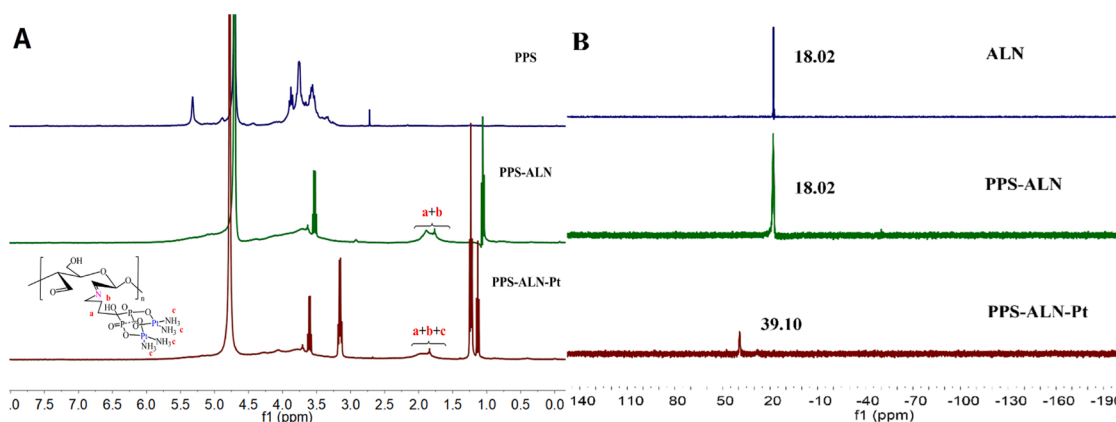


Fig. 1. (A) ^1H NMR spectra of PPS, PPS-ALN and PPS-ALN-Pt in D_2O ; (B) ^{31}P NMR spectra of ALN ($\text{DMSO}-d_6$), PPS-ALN and PPS-ALN-Pt (D_2O).

approximately 18.02 ppm. The P—CP— signal peak of ALN also appeared in the ^{31}P NMR spectra of PPS-ALN conjugates at approximately 18.02 ppm. As shown in Fig. 1(B), the signal of ^{31}P NMR spectra was about 39.10 ppm, which belonged to the two phosphorus atoms in the bisphosphonate group of PPS-ALN-Pt conjugates. They were magnetically equivalent and transferred to lower field. The low-field displacement of the phosphorus nuclei at approximately 39.10 ppm was caused by the coordination of phosphonate oxygen with the metal platinum. In general, the measurements of FT-IR combined with NMR spectra confirmed that PPS-ALN and PPS-ALN-Pt conjugates were successfully synthesized.

3.4. DS of the phosphate radical of PPS-ALN-Pt conjugates

According to standard curve regression equation of phosphate anion in Fig. S2 ($Y = 0.0732 X + 0.0445$, $R^2 = 0.9997$), the content of PO_4^{3-} from PPS-ALN-Pt conjugates was calculated as 10.95 %. Owing to two phosphate radicals are contained in ALN, the content of PO_4^{3-} should be adjusted to 5.47 %. Therefore, the contents of the phosphate group $-\text{PO}_3\text{H}_2$ was accordingly 4.66 %. The DS of $-\text{PO}_3\text{H}_2$ in PPS-ALN-Pt conjugates was calculated as 0.139 under Eq. (1). On the other hand, it was exactly indicated that phosphorylation had been successfully carried out.

3.5. TGA analysis

Thermal stability of these samples was investigated by a thermal gravimetric instrument as shown in Fig. S3. The modification improved the thermal stability of PPS-ALN-Pt copolymer. Compared with the pure *Portulaca oleracea* polysaccharides, the first mass loss around 52–110 °C may be the loss of water. Followed by the mass loss of the phosphate group and coordination bond was the region of near 170–400 °C, and its decomposition speed was accelerated. Finally, the carbon structure of the polysaccharide ring [53] could be decomposed at 400–850 °C. Fig. S3(b) showed TGA curves of ALN, in which the first step mass loss of ALN around 110–140 °C was due to loss crystal water. The second stage at approximately 245–500 °C, corresponding to 30 % mass loss, was the primary thermal decomposition owing to decomposition of phosphate. The final remaining mass of ALN was about 49 % of the initial mass, which had the best thermal stability among these samples. After grafting with ALN and Pt, the skeleton structure of PPS became more stable which made it have better stability at high temperature.

3.6. XRD analysis

X-ray powder diffraction (XRD) spectra was used to reflect the crystalline degree of powder samples [54]. The diffraction patterns of PPS, PPS-ALN and PPS-ALN-Pt conjugates were measured using X-ray

diffractometer with the 2θ ranges of 5–80° as showed in Fig. 2. PPS had only a broad diffraction peak at $2\theta \approx 19.72^\circ$, suggesting that PPS was powder diffraction patterns with typical amorphous materials amorphous in nature. Previous studies had indicated that polysaccharides with amorphous state properties were more stable [55]. The diffraction pattern of the PPS-ALN and PPS-ALN-Pt conjugates had no distinct peaks and emerged a dispersion state. The results demonstrated that the modified polysaccharide molecule not only underwent a chemical structure change, but the cross-linking of the structure led to dispersion state.

3.7. Antioxidant activity analysis

Portulaca oleracea polysaccharides were studied for the potential antioxidant or scavenging activities [56]. Therefore, the antioxidant test was used to detect whether the modified products still possessing the ability to scavenge free radicals. The antioxidant capacities of PPS, ALN, PPS-ALN and PPS-ALN-Pt conjugates at measurement concentrations from 0 to 0.10 or 0 to 0.20 mg/mL were estimated by most frequently used free radical scavenging assays (ABTS and DPPH methods) presented in Fig. 3. The ABTS and DPPH scavenging free radical effect of PPS-ALN conjugates increased with the increase of concentration up to 0.1 mg/mL (> 89.5 %) and 0.19 mg/mL (> 77.1 %), respectively.

Moreover, the scavenging activities of PPS-ALN and PPS-ALN-Pt conjugates increased significantly with the increase of concentration in DPPH radical scavenging assay. As shown in Fig. 3, PPS-ALN-Pt conjugates showed the ability of scavenging free radicals in different rules, which still had certain antioxidant capacity. The scavenging free

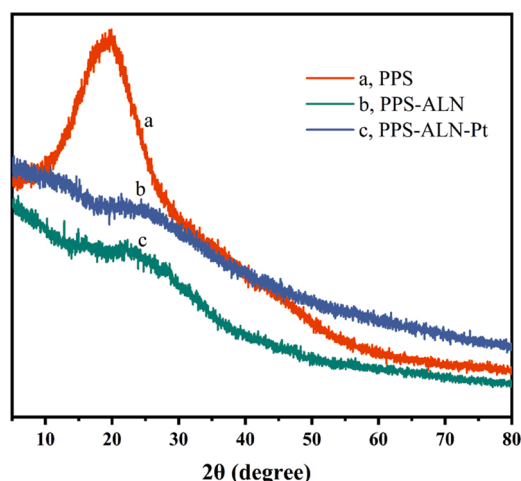


Fig. 2. XRD patterns of PPS (a), PPS-ALN (b) and PPS-ALN-Pt (c).

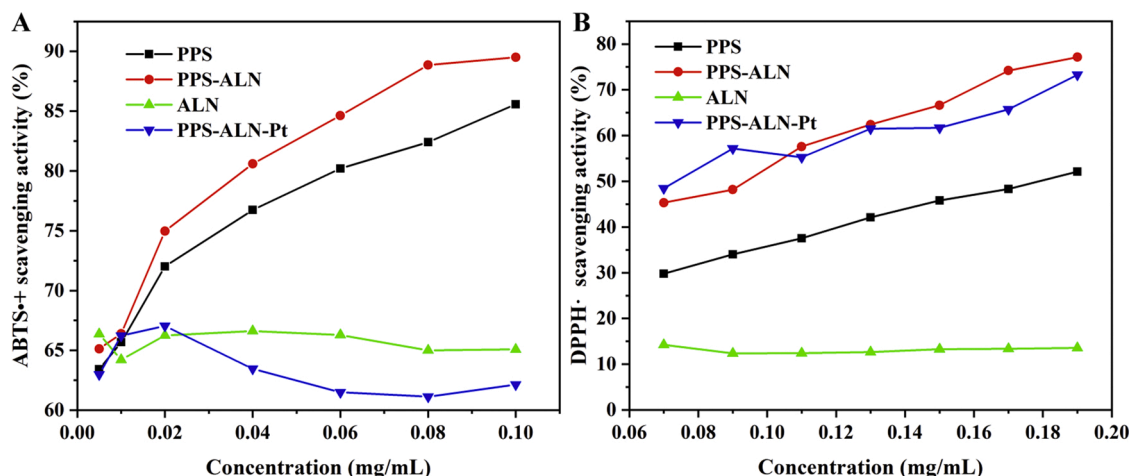


Fig. 3. ABTS (A) and DPPH (B) radical scavenging activities of PPS, ALN, PPS-ALN and PPS-ALN-Pt.

radical assays results of PPS had the hydrogen-donating capacity of antioxidants. The hydroxyl groups of ALN provided a hydrogen supply capacity, which made PPS-ALN conjugates stronger antioxidant. Under the combined coordination of Pt and PPS-ALN conjugates made the decrease of hydroxyl groups of PPS-ALN-Pt conjugates which kept relatively stable antioxidant activity.

3.8. Cytotoxicity evaluation

The effect of PPS, ALN, cisplatin, PPS-ALN and PPS-ALN-Pt conjugates on cell viability was detected by MTT experiment. HeLa, MCF-7, LO-2, and A549 cells were respectively incubated with PPS, ALN, cisplatin, PPS-ALN and PPS-ALN-Pt conjugates, the cells viabilities of them were then detected. The IC_{50} values of these sample against HeLa, MCF-7, LO-2, and A549 cells were depicted in Fig. 4. PPS had a lower antiproliferative effect on HeLa and LO-2 cells compared with MCF-7, and A549 cells, giving IC_{50} values of PPS 1113.3, 1113.4, 867.1 and 481.4 $\mu\text{g/mL}$ for HeLa, LO-2, MCF-7, and A549 cells, respectively.

Nevertheless, PPS-ALN-Pt conjugates had approximately the same IC_{50} values, which were 284.29, 262.1 and 233.8 $\mu\text{g/mL}$, respectively, for HeLa, MCF-7 and A549 cells. The results of PPS-ALN-Pt conjugates confirmed that they had a particular effect on cancer cells. PPS-ALN-Pt conjugates was more cytotoxic than PPS, ALN, and PPS-ALN conjugates toward the tested tumor cells. The P=O of phosphate radicals of PPS-ALN conjugates can be coordinated with the amino group on cisplatin but not be exposed to the outside, so the PPS-ALN-Pt conjugates did not exhibit selectivity.

On the other hand, IC_{50} values of cisplatin to HeLa, MCF-7, LO-2, and A549 cells were 0.087, 3.15, 1.23, 5.88 $\mu\text{g/mL}$ (0.29, 10.49, 4.10, 19.57 μM), confirmed that cisplatin had a strong inhibitory effect on cell growth. The IC_{50} values of ALN to HeLa and LO-2 cells were smaller than MCF-7 and A549 cells, moreover, IC_{50} values of HeLa cells were the smallest that is ALN had the most toxic for HeLa cells. The precursor of cisplatin coordinated with PPS-ALN formed PPS-ALN-Pt conjugates, which had similar IC_{50} values in HeLa and LO-2 cells. PPS-ALN-Pt conjugates had a similar effect to inhibit cells proliferation for HeLa, MCF-7, LO-2, and A549 cells. It was impersonally indicated that the antitumor activity of cisplatin remained when the precursor was coordinated with PPS-ALN conjugates containing carrier. However, the IC_{50} values of PPS-ALN-Pt conjugates were higher than cisplatin among four cell lines, which was related to the amount of grafted cisplatin hydrate in the conjugates.

3.9. Plasmid DNA interaction with PPS-ALN-Pt conjugates

The unwrapping of the closed circular and supercoiled pUC19 plasmid DNA by interacting with PPS-ALN-Pt conjugates were detected using an electrophoretic mobility shift experiment. The plasmid pUC19 had a double-stranded shape and existed as a supercoiled structure. Since strand break was introduced, the superhelix form of DNA was broken into the nicked circular or the linear form. When one of the strands was severed, the super curl form would loosen, forming a notched circular structure. When both strands were split, a line shape would emerge. DNA molecules with the same molecular weight needed

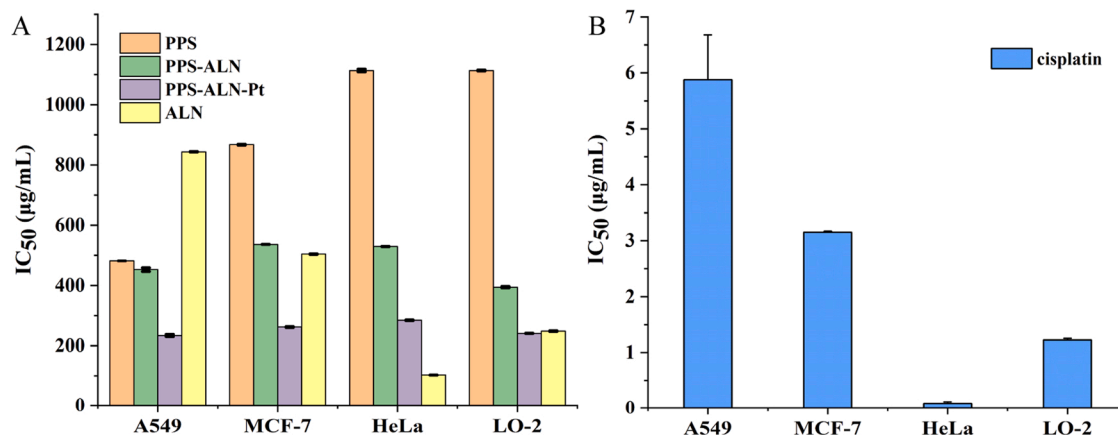


Fig. 4. The IC_{50} value of A549, MCF-7, HeLa and LO-2 cells treated with PPS, ALN, PPS-ALN and PPS-ALN-Pt (A) and A549, MCF-7, HeLa and LO-2 cells treated with cisplatin (B).

to migrate differently according to their spatial structure of the DNA molecules during electrophoresis [47]. The electrophoretic migration speed of the closed-loop helix structure was the fastest, followed by the linear structure and the open-loop structure. In the wake of PPS-ALN-Pt conjugates concentration, the migration rate of DNA after treating with the drug was slightly delayed compared with that of free supercoiled DNA as seen in Fig. S4. It brought to light conclusion that the helicity of DNA could be interfered by PPS-ALN-Pt conjugates, which led to the change of DNA replication mechanisms and the processing disruption of this DNA eventually triggered cell apoptosis.

3.10. Nuclear staining

Fluorescence microscopy was used to analyze the nuclear morphological changes of HeLa cells staining with Hoechst 33,342, which confirmed the apoptosis of cells [57]. The ability of PPS, PPS-ALN and PPS-ALN-Pt conjugates to induce apoptosis was studied. The nuclear morphology of HeLa cells, after incubated with PPS, PPS-ALN and PPS-ALN-Pt conjugates at different concentrations for 24 h, was observed by a fluorescence microscope. As depicted in Fig. 5, The nucleus of HeLa cells in the control group was in weak blue fluorescence with a regular round outline. The nucleus morphology of HeLa cells treated with PPS at IC₅₀ value resembled that of the control group, illustrating that PPS had no effect on HeLa cells nucleation. However, the nucleus morphology of HeLa cells incubated with cisplatin, PPS-ALN and PPS-ALN-Pt conjugates at different concentrations displayed condensation, nucleus shrinkage, and even nuclear fragmentation. On the other hand, the nucleus morphology changed of HeLa cells treated with PPS-ALN-Pt conjugates was more visible. In a nutshell, PPS-ALN-Pt conjugates had a significant induction effect on apoptosis of HeLa cells having a concentration-dependent manner.

3.11. The distribution of CRT in HeLa cells

Calcium reticulin (CRT), a highly conserved multifunctional protein, is widely distributed in the cell nucleus, endoplasmic reticulum and cell membrane [58]. Experimental data displayed that CRT was firmly related to the occurrence and development of tumors. CRT was transferred to the surface of the cell membrane, aiming to mediate the immunogenicity death of tumor cells [59]. So, it played an essential role in regulating the immunogenicity of tumor cells. CRT can be synthesized in normal cells, apoptotic cells, tumor cells and partial drug treatment

cells. The expression of calreticulin in HeLa cells was studied by immunofluorescence assay. When drugs stimulated cells to undergo the process of apoptosis, CRT transferred from intracellular to the cell membrane. As shown in Fig. 6, DAPI staining (blue fluorescence) assisted in locating the nucleus and the antibody labelled CRT (green fluorescence) of HeLa cells in the control group also expressed. The expression CRT of HeLa cells after treated with PPS, PPS-ALN and PPS-ALN-Pt conjugates was in turn increased. CRT induced by cisplatin was slightly higher than control cells. Moreover, the induction of CRT by PPS-ALN-Pt conjugates also moderately increased when compared to that of control cells. Therefore, PPS-ALN-Pt conjugates played a particular role in regulating the immunogenicity of HeLa tumor cells and also induced apoptosis correspondingly.

3.12. Cellular Pt uptake and DNA platinization

The cellular accumulation of Pt in HeLa cells was detected by ICP-MS. As shown in Table 1, PPS-ALN-Pt conjugates have a higher platinum binding protein effect on HeLa cells than cisplatin, due to the excellent biocompatibility of polysaccharides. Generally, the reported DNA platinum was approximately 1%. Due to the different factors such as the action time, cell type, drug concentration, etc., the ability of cisplatin and PPS-ALN-Pt conjugates to platinate nuclear DNA in this experiment was high. By formula conversion calculation, the ability of PPS-ALN-Pt to platinate nuclear DNA in cells was higher than cisplatin from the cellular uptake data of Table 1. On the basis of above studies, PPS-ALN-Pt conjugates displayed slightly higher platinization ability than cisplatin, which was attributed to the higher cellular uptake.

4. Conclusion

In summary, a sugar ring carrier containing biphosphate group bridging ligand was rationally designed and synthesized. The coupling Pt complexes of PPS-ALN conjugates were characterized by FT-IR, ¹H NMR, ³¹P NMR, XRD, TGA analysis. The results of PPS-ALN-Pt conjugates had good thermal stability. In terms of scavenging active radicals, PPS-ALN conjugates were significantly more potent than PPS, while the antioxidant activity of PPS-ALN-Pt conjugates was kept relatively stable, indicating that it had a certain extent antioxidant capacity to reduce the occurrence of some inflammation. MTT assay results illustrated that PPS-ALN-Pt conjugates had lower cytotoxicity in comparison with cisplatin and ALN against HeLa cells. PPS-ALN-Pt conjugates interfered

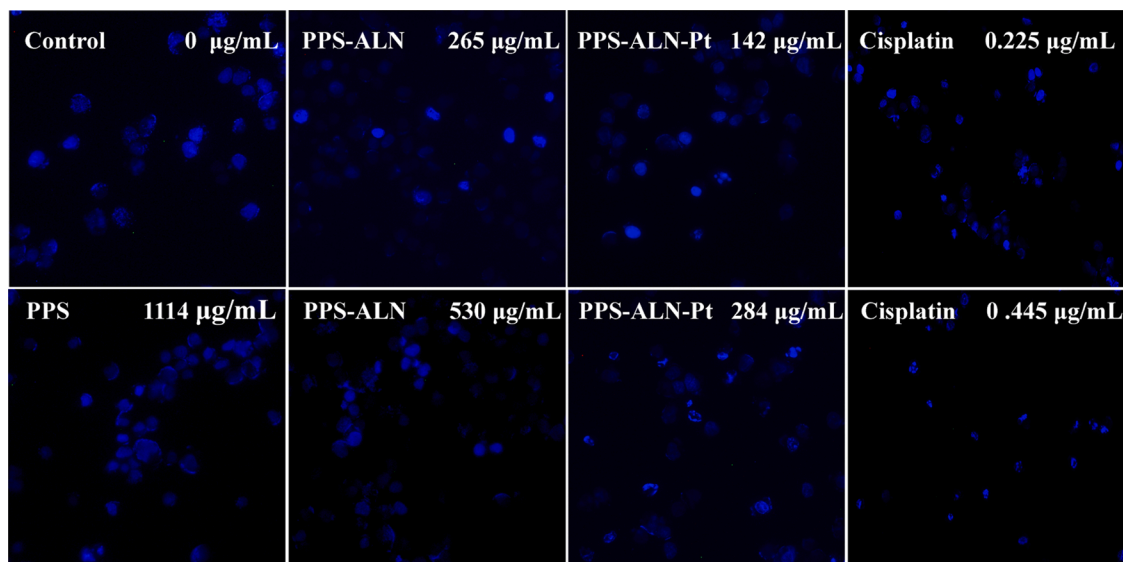


Fig. 5. Morphological alterations of the nuclei of HeLa cells after incubation with PPS (1114 µg/mL), PPS-ALN (265 and 530 µg/mL), PPS-ALN-Pt (142 and 284 µg/mL) and cisplatin (0.225 and 0.445 µg/mL) for 24 h and staining with Hoechst 33342.

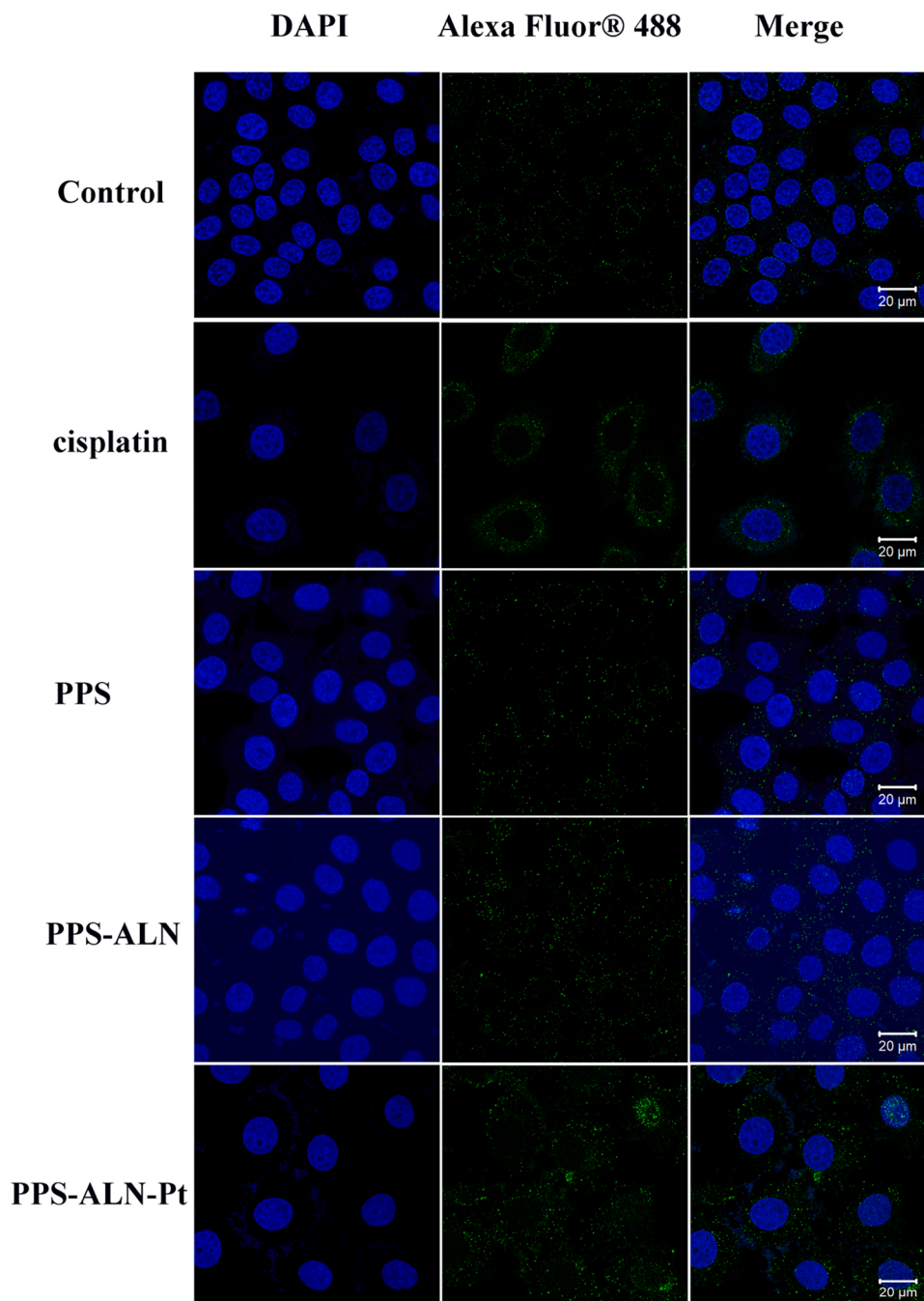


Fig. 6. The distribution of calreticulin in HeLa cells after incubation with control, cisplatin (0.0871 $\mu\text{g/mL}$), PPS (1114 $\mu\text{g/mL}$), PPS-ALN (530 $\mu\text{g/mL}$) and PPS-ALN-Pt (284 $\mu\text{g/mL}$) for 24 h. Scale bars: 20 μm .

Table 1

Cellular uptake of Pt and platinization of cellular DNA in HeLa cells after exposure to cisplatin (45 $\mu\text{g/mL}$) and PPS-ALN-Pt (284 $\mu\text{g/mL}$) for 24 h ^a.

	PPS-ALN-Pt	cisplatin
ng Pt/mg Protein	191.76 \pm 2.96	8.83 \pm 0.21
ng Pt/ μg DNA	16.00 \pm 0.50	7.82 \pm 0.11

^a Average of three measurements.

with the helicity of DNA by gel electrophoresis assay and possess binding ability with DNA by cellular uptake assay. We explored that PPS-ALN-Pt conjugates played a significant role in regulating immunogenicity and inducing apoptosis of tumor cells by immunofluorescence assay.

Overall, the easily prepared PPS-ALN-Pt conjugates could be a promising strategy for anti-tumor pharmacotherapy.

CRediT authorship contribution statement

Qianqian Han: Conceptualization, Investigation, Methodology, Writing - original draft. **Lirong Huang:** Resources, Conceptualization, Investigation. **Ying Wang:** Visualization, Investigation. **Shixin Sun:** Visualization, Investigation. **Hao Huang:** Visualization, Investigation. **Fei Li:** Visualization, Investigation. **Fangtian Wang:** . **Ligen Chen:** Visualization, Investigation. **Hongmei Zhang:** Writing - review & editing, Supervision. **Yanqing Wang:** Writing - review & editing, Supervision.

Declaration of Competing Interest

The authors declare no conflict of interest.

Acknowledgement

This work was supported by the National Natural Science Foundation of China (Project No. 21571154), the "Six Talent Peaks Project" in Jiangsu Province, the Jiangsu Fundament of "Qinglan Project" and "333 Project".

Appendix A. Supplementary data

Supplementary material related to this article can be found, in the online version, at doi:<https://doi.org/10.1016/j.colsurfb.2021.111628>.

References

- [1] L. Kelland, The resurgence of platinum-based cancer chemotherapy, *Nat. Rev. Cancer* 7 (2007) 573–584.
- [2] T.C. Johnstone, K. Suntharalingam, S.J. Lippard, The next generation of platinum drugs: targeted Pt(II) agents, nanoparticle delivery, and Pt(IV) prodrugs, *Chem. Rev.* 116 (2016) 3436–3486.
- [3] H.Y. Yu, Z.H. Tang, D.W. Zhang, W.T. Song, Y. Zhang, Y. Yang, Z. Ahmad, X. S. Chen, Pharmacokinetics, biodistribution and in vivo efficacy of cisplatin loaded poly(l-glutamic acid)-g-methoxy poly(ethylene glycol) complex nanoparticles for tumor therapy, *J. Control. Release* 205 (2015) 89–97.
- [4] S. Altmann, K. Choroba, M. Skonieczna, D. Zygadlo, M. Raczynska-Szajgin, A. Maroń, J.G. Malecki, A. Szlapa-Kula, M. Tomczyk, A. Ratuszna, B. Machura, A. Szurko, Platinum(II) coordination compounds with 4'-pyridyl functionalized 2,2':6',2''-terpyridines as an alternative to enhanced chemotherapy efficacy and reduced side-effects, *J. Inorg. Biochem.* 201 (2019), 110809.
- [5] P.G. Avaji, H.I. Joo, J.H. Park, K.S. Park, Y.J. Jun, H.J. Lee, Y.S. Sohn, Synthesis and properties of a new micellar polyphosphazene-platinum(II) conjugate drug, *J. Inorg. Biochem.* 140 (2014) 45–52.
- [6] Michal Bachar, Amitai Mandelbaum, Irina Portnaya, Hadas Perlstein, Simcha Even-Chen, Yechezkel Barenholz, Dganit Danino, Development and characterization of a novel drug nanocarrier for oral delivery, based on self-assembled β -casein micelles, *J. Control. Release* 160 (2012) 164–171.
- [7] H.Y. Li, K.L. Liu, Q.Q. Sang, G.R. Williams, J.Z. Wu, H.J. Wang, J.R. Wu, L.-M. Zhu, A thermosensitive drug delivery system prepared by blend electrospinning, *Colloids Surf. B* 159 (2017) 277–283.
- [8] M. Zhang, X.L. Guo, M.F. Wang, K.H. Liu, Tumor microenvironment-induced structure changing drug/gene delivery system for overcoming delivery-associated challenges, *J. Control. Release* 323 (2020) 203–224.
- [9] J. Bugno, H.-j. Hsu, S. Hong, Recent advances in targeted drug delivery approaches using dendritic polymers, *Biomater. Sci.* 3 (2015) 1025–1034.
- [10] X.J. Zhang, S.W. Niu, G.R. Williams, J.R. Wu, X. Chen, H. Zheng, L.-M. Zhu, Dual-responsive nanoparticles based on chitosan for enhanced breast cancer therapy, *Carbohydr. Polym.* 221 (2019) 84–93.
- [11] K.B. Huang, F.Y. Wang, X.M. Tang, H.W. Feng, Z.F. Chen, Y.C. Liu, Y.N. Liu, H. Liang, Organometallic gold(III) complexes similar to tetrahydroisoquinoline induce ER-stress-mediated apoptosis and pro-Death autophagy in A549 cancer cells, *J. Med. Chem.* 61 (2018) 3478–3490.
- [12] F. Chen, G. Huang, Application of glycosylation in targeted drug delivery, *Eur. J. Med. Chem.* 182 (2019), 111612.
- [13] H.H. Xiao, L.S. Yan, E.M. Dempsey, W.T. Song, R.G. Qi, W.L. Li, Y.B. Huang, X. B. Jing, D.F. Zhou, J.X. Ding, X.S. Chen, Recent progress in polymer-based platinum drug delivery systems, *Prog. Polym. Sci.* 87 (2018) 70–106.
- [14] A.M. Alshehri, O.C. Wilson, B. Dahal, J. Philip, X.L. Luo, C.B. Raub, Magnetic nanoparticle-loaded alginate beads for local micro-actuation of in vitro tissue constructs, *Colloids Surf. B* 159 (2017) 945–955.
- [15] S. Indoria, V. Singh, M.-F. Hsieh, Recent advances in theranostic polymeric nanoparticles for cancer treatment: a review, *Int. J. Pharmaceut.* 582 (2020), 119314.
- [16] J.J. Diao, F. Bai, Y. Wang, Q.Q. Han, X. Xu, H.M. Zhang, Q. Luo, Y.Q. Wang, Engineering of pectin-dopamine nano-conjugates for carrying ruthenium complex: a potential tool for biomedical applications, *J. Inorg. Biochem.* 191 (2019) 135–142.
- [17] A. Travan, F. Scognamiglio, M. Borgogna, E. Marsich, I. Donati, L. Tarusha, M. Grassi, S. Paoletti, Hyaluronan delivery by polymer demixing in polysaccharide-based hydrogels and membranes for biomedical applications, *Carbohydr. Polym.* 150 (2016) 408–418.
- [18] F. Roig, M. Blanzat, C. Solans, J. Esquena, M.J. García-Celma, Hyaluronan based materials with cationic sugar-derived surfactants as drug delivery systems, *Colloids Surf. B* 164 (2018) 218–223.
- [19] X. Zhang, D. Liu, F. Lv, B. Yua, Y. Shen, H. Cong, Recent advances in ruthenium and platinum based supramolecular coordination complexes for antitumor therapy, *Colloids Surf. B* 182 (2019), 110373.
- [20] L. He, J.X. Xu, X. Cheng, M. Sun, B. Wei, N.C. Xiong, J.Y. Song, X. Wang, R.P. Tang, Hybrid micelles based on Pt (IV) polymeric prodrug and TPGS for the enhanced cytotoxicity in drug-resistant lung cancer cells, *Colloids Surf. B* 195 (2020), 111256.
- [21] X. Wang, C.C. Yang, Y.J. Zhang, X. Zhen, W. Wu, X.Q. Jiang, Delivery of platinum (IV) drug to subcutaneous tumor and lung metastasis using bradykinin-potentiating peptide-decorated chitosan nanoparticles, *Biomaterials* 35 (2014) 6439–6453.
- [22] T. Moreira, R. Francisco, E. Comsa, S. Duban-Deweer, V. Labas, A. Teixeira-Gomes, L. Combes-Soia, F. Marques, A. Matos, A. Favrelle, C. Rousseau, P. Zinck, P. Falson, H. Garcia, A. Preto, A. Valente, Polymer "ruthenium-cyclopentadienyl" conjugates-New emerging anti-cancer drugs, *Eur. J. Med. Chem.* 168 (2019) 373–384.
- [23] E.S. Elkhatay, S.R. Ibrahim, M.A. Aziz, Portulene, a new diterpene from *Portulaca oleracea* L., *J. Asian Nat. Prod. Res.* 10 (2008) 1039–1043.
- [24] Y.-P. Li, L.-H. Yao, G.-J. Wu, X.-F. Pi, Y.-C. Gong, R.-S. Ye, C.-X. Wang, Antioxidant activities of novel small-molecule polysaccharide fractions purified from *Portulaca oleracea* L., *Food Sci. Biotechnol.* 23 (2014) 2045–2052.
- [25] C.-X. Dong, K. Hayashi, J.-B. Lee, T. Hayashi, Characterization of structures and antiviral effects of polysaccharides from *Portulaca oleracea* L., *Chem. Pharm. Bull.* 58 (2010) 507–510.
- [26] Y.N. Georgiev, M.H. Ognyanov, H. Kiyohara, T.G. Batsalova, B.M. Dzhambazov, M. Ciz, P.N. Denev, H. Yamada, B.S. Paulsen, O. Vasicek, A. Lojek, H. Barsett, D. Antonova, M.G. Kratchanova, Acidic polysaccharide complexes from purslane, silver linden and lavender stimulate Peyer's patch immune cells through innate and adaptive mechanisms, *Int. J. Biol. Macromol.* 105 (2017) 730–740.
- [27] K.-B. Oh, I.-M. Chang, K.-J. Hwang, W. Mar, Detection of antifungal activity in *Portulaca oleracea* by a single-cell bioassay system, *Phytother. Res.* 14 (2000) 329–332.
- [28] H. Shen, G. Tang, G. Zeng, Y.J. Yang, X.W. Cai, D.L. Li, H.C. Liu, N.X. Zhou, Purification and characterization of an antitumor polysaccharide from *Portulaca oleracea* L., *Carbohydr. Polym.* 93 (2013) 395–400.
- [29] R. Zhao, X. Gao, Y.P. Cai, X.Y. Shao, G.Y. Jia, Y.L. Huang, X.G. Qin, J.W. Wang, X. L. Zheng, Antitumor activity of *Portulaca oleracea* L. Polysaccharides against cervical carcinoma in vitro and in vivo, *Carbohydr. Polym.* 96 (2013) 376–383.
- [30] Y.Q. Li, Y.K. Hu, S.J. Shi, L. Jiang, Evaluation of antioxidant and immunoenhancing activities of Purslane polysaccharides in gastric cancer rats, *Int. J. Biol. Macromol.* 68 (2014) 113–116.
- [31] H. Shen, G. Tang, G. Zeng, Y.J. Yang, X.W. Cai, D.L. Li, H.C. Liu, N.X. Zhou, Purification and characterization of an antitumor polysaccharide from *Portulaca oleracea* L., *Carbohydr. Polym.* 93 (2013) 395–400.
- [32] J. Maia, R.A. Carvalho, J.F.J. Coelho, P.N. Simões, M.H. Gil, Insight on the periodate oxidation of dextran and its structural vicissitudes, *Polymer* 52 (2011) 258–265.
- [33] S. Oliver, E. Yee, M. Kavallaris, O. Vittorio, C. Boyer, Water soluble antioxidant dextran-queretin conjugate with potential anticancer properties, *Macromol. Biosci.* 18 (2018), 1700239.
- [34] S. Martwiset, A.E. Koh, W. Chen, Nonfouling characteristics of dextran-containing surfaces, *Langmuir* 22 (2006) 8192–8196.
- [35] D. Li, J.X. Ding, X.L. Zhuang, L. Chen, X.S. Chen, Drug binding rate regulates the properties of polysaccharide prodrugs, *J. Mater. Chem. B* 4 (2016) 5167–5177.
- [36] X.R. Feng, D. Li, J.D. Han, X.L. Zhuang, J.X. Ding, Schiff base bond-linked polysaccharide-doxorubicin conjugate for upregulated cancer therapy, *Mater. Sci. Eng. C* 76 (2017) 1121–1128.
- [37] N.U. Deshpande, M. Jayakannan, Cisplatin-stitched polysaccharide vesicles for synergistic Cancer therapy of triple antagonistic drugs, *Biomacromolecules* 18 (2017) 113–126.
- [38] Y.L. He, M. Ye, L.Y. Jing, Z.Z. Du, M. Surahio, H.M. Xu, J. Li, Preparation, characterization and bioactivities of derivatives of an exopolysaccharide from *Lachnum*, *Carbohydr. Polym.* 117 (2015) 788–796.
- [39] M. Zhang, N.N. Su, Q.L. Huang, Q. Zhang, Y.F. Wang, J.L. Li, M. Ye, Phosphorylation and antiaging activity of polysaccharide from *Trichosanthin* peel, *J. Food Drug Anal.* 25 (2017) 976–983.
- [40] R. Re, N. Pellegrini, A. Proteggente, A. Pannala, M. Yang, C. Rice-Evans, Antioxidant activity applying an improved ABTS radical cation decolorization assay, *Free Radic. Biol. Med.* 26 (1999) 1231–1237.
- [41] F. Chen, G.L. Huang, Extraction, derivatization and antioxidant activity of bitter gourd polysaccharide, *Int. J. Biol. Macromol.* 141 (2019) 14–20.
- [42] Y. Wang, Q.Q. Han, F. Bai, Q. Luo, M.L. Wu, G. Song, H.M. Zhang, Y.Q. Wang, The assembly and antitumor activity of lycium barbarum polysaccharide-platinum-based conjugates, *J. Inorg. Biochem.* 205 (2020), 111001.
- [43] K.R. Jeyalakshmi, Y. Arun, N.S.P. Bhuvanesh, P.T. Perumal, A. Sreekanth, R. Karvemu, DNA/protein binding, DNA cleavage, cytotoxicity, superoxide radical scavenging and molecular docking studies of copper(II) complexes containing N-benzyl-N'-aryl-N''-benzoylguanidine ligands, *Inorg. Chem. Front.* 2 (2015) 780–798.
- [44] J.J. Ou, Y. Peng, W.W. Yang, Y. Zhang, J. Hao, F. Li, Y.R. Chen, Y. Zhao, X. Xie, S. Wu, L. Zha, X. Luo, G.F. Xie, L.T. Wang, W. Sun, Q. Zhou, J.J. Li, H.J. Liang, ABHD5 blunts the sensitivity of colorectal cancer to fluorouracil via promoting autophagic uracil yield, *Nat. Commun.* 10 (2019) 1078.
- [45] S.R. Zhang, H. Yuan, Y. Guo, K. Wang, X.Y. Wang, Z.J. Guo, Towards rational design of RAD51-targeting prodrugs: platinum^{IV}-artesanate conjugates with enhanced cytotoxicity against BRCA-proficient ovarian and breast cancer cells, *Chem. Commun.* 54 (2018) 11717–11720.
- [46] Y. Guo, Y.F. He, S.D. Wu, S.R. Zhang, D.F. Song, Z.Z. Zhu, Z.J. Guo, X.Y. Wang, Enhancing cytotoxicity of a monofunctional platinum complex via a Dual-DNA-Damage approach, *Inorg. Chem.* 58 (2019) 13150–13160.
- [47] B.P. Purcell, D. Lobb, M.B. Charati, S.M. Dorsey, R.J. Wade, K.N. Zellars, H. Doviak, S. Pettaway, C.B. Logdon, J.A. Shuman, Injectable and bioresponsive

- hydrogels for on-demand matrix metalloproteinase inhibition, *Nat. Mater.* 13 (2014) 653–661.
- [49] T. Qiu, X.J. Ma, M. Ye, R.Y. Yuan, Y.N. Wu, Purification, structure, lipid lowering and liver protecting effects of polysaccharide from *Lachnum YM281*, *Carbohydr. Polym.* 98 (2013) 922–930.
- [50] Y.J. Huang, Y.F. He, Z.Y. Huang, Y.L. Jiang, W.J. Chu, X.Q. Sun, L.F. Huang, C. S. Zhao, Coordination self-assembly of platinum-bisphosphonate polymer-metal complex nanoparticles for cisplatin delivery and effective cancer therapy, *Nanoscale* 9 (2017) 10002–10019.
- [51] N. Margiotta, R. Ostuni, V. Gandin, C. Marzano, S. Piccinonna, G. Natile, Synthesis, characterization, and cytotoxicity of dinuclear platinum-bisphosphonate complexes to be used as prodrugs in the local treatment of bone tumours, *Dalton Trans.* (2009) 10904–10913.
- [52] T.G. Appleton, J.R. Hall, S.F. Ralph, C.S.M. Thompson, Reactions of platinum(II) aqua complexes. 2. Platinum-195 NMR study of reactions between the tetraaquaplutonium(II) cation and chloride, hydroxide, perchlorate, nitrate, sulfate, phosphate, and acetate, *Inorg. Chem.* 23 (1984) 3521–3525.
- [53] E.F. Lessa, M.S. Gularte, E.S. Garcia, A.R. Fajardo, Orange waste: a valuable carbohydrate source for the development of beads with enhanced adsorption properties for cationic dyes, *Carbohydr. Polym.* 157 (2017) 660–668.
- [54] E.P. Schokker, J.S. Church, J.P. Mata, E.P. Gilbert, A. Puvanenthiran, P. Udabage, Reconstitution properties of micellar casein powder: effects of composition and storage, *Internat. Dairy J.* 21 (2011) 877–886.
- [55] H. Munir, M. Shahid, F. Anjum, D. Mudgil, Structural, thermal and rheological characterization of modified *Dalbergia sissoo* gum-A medicinal gum, *Int. J. Biol. Macromol.* 84 (2016) 236–245.
- [56] Y.G. Chen, Z.J. Shen, X.P. Chen, Evaluation of free radicals scavenging and immunity-modulatory activities of Purslane polysaccharides, *Int. J. Biol. Macromol.* 45 (2009) 448–452.
- [57] X.B. Zhao, L. Liu, X.R. Li, J. Zeng, X. Jia, P. Liu, Biocompatible graphene oxide nanoparticle-based drug delivery platform for tumor microenvironment-responsive triggered release of doxorubicin, *Langmuir* 30 (2014) 10419–10429.
- [58] S. Johnson, M. Michalak, M. Opas, P. Eggleton, The ins and outs of calreticulin: from the ER lumen to the extracellular space, *Trends Cell Biol.* 11 (2001) 122–129.
- [59] A. Tesniere, L. Apetoh, F. Ghiringhelli, N. Joza, T. Panaretakis, O. Kepp, F. Schlemmer, L. Zitvogel, G. Kroemer, Immunogenic cancer cell death: a key-lock paradigm, *Curr. Opin. Immunol.* 20 (2008) 504–511.